Supporting Information

Targeted delivery and release of Doxorubicin using pH-responsive and self-assembling copolymer

Kaizong Huang[a], Lingli Zhu[a], Yunke Wang[a], Ran Mo[b], Zichun Hua[a,b*]

[a] The State Key Laboratory of Pharmaceutical Biotechnology, School of Life Sciences, Nanjing University, Nanjing, 210046, P.R. China. E-mail: zchua@nju.edu.cn.

[b] State Key Laboratory of Natural Medicines, China Pharmaceutical University, 24 Tongjia Xiang, Nanjing 210009, P. R. China.

Supplementary figures

1. **Figure S1.** MALDI-TOF analyzed molecular weight of ELP[V_5-70](a), PEG-ELP[V_5-70] (b), ELP[VH_4-70](c) and PEG-ELP[VH_4-70] (d)
2. **Figure S2.** ANS analyzed hydrophobicity of PEG, ELP and PEG-ELP.
3. **Supplemental Figure 2.** Material properties of histidine-rich ELPs and PEG-ELP. turbidimetry (A350) was measured over a range of pH.
4. **Figure S4.** Hydraulic radius was measured with different pH, presenting 50μM $ZnCl_2$ (37 ^oC).
5. **Figure S5.**Intracellular release of DOX on CT-26 cells at different time (1, 4 h) observed by fluorescence microscopy.
6. **Figure S6.** Cellular uptake of PEG-ELP/DOX on CT-26 cells.
7. **Figure S7.** Effects of PEG-ELP/DOX and free DOX viability of CT-26.
8. **Figure S8.** Effects of PEG-ELP viability of CT-26. Cells were incubated with increasing concentrations of PEG-ELP in culture medium for 24 h. The proliferative response was then assessed by MTT.
9. **Figure S9**. Plasma concentration-time profiles of DOX following i.v administration of Free DOX, PEG-ELP[V_5-70]/DOX and PEG-ELP[VH_4-70]/DOX (5mg/kg).
10. **Figure S10.** *Ex vivo* fluorescence imaging of the tumor and normal tissues harvested from the euthanized tumor-bearing BALB/c mice injection with different 797 fluorescent agent formulations.

11. **Figure S11.** Quantification of fluorescent signal intensities of excised organs from mice at 24 h post injection. The data was recorded as total photons per centimeter squared per steradian (p/s/cm^2/sr).
12. **Figure S12.** Animals were sacrificed 14 days after withdrawing administration and tumors were harvested and imaged.
13. **Figure S13.** Tumor sections were immunostained with TUNEL staining for tumor cell apoptosis after treatment with different formulations.
14. **Figure S14**. Hematoxylin-eosin (H&E) staining examination of tumor from the treated mice.
15. **Figure S15.** Hematoxylin-eosin (H&E) staining examination of liver from the treated mice.
16. **Figure S16.** Body weight of each mouse in five groups was measured every three day. Results are expressed as mean ± S.D.
17. **Figure S17.** *In vitro* average diameter distribution of PEG-ELP[VH_4-70]/DOX over time.

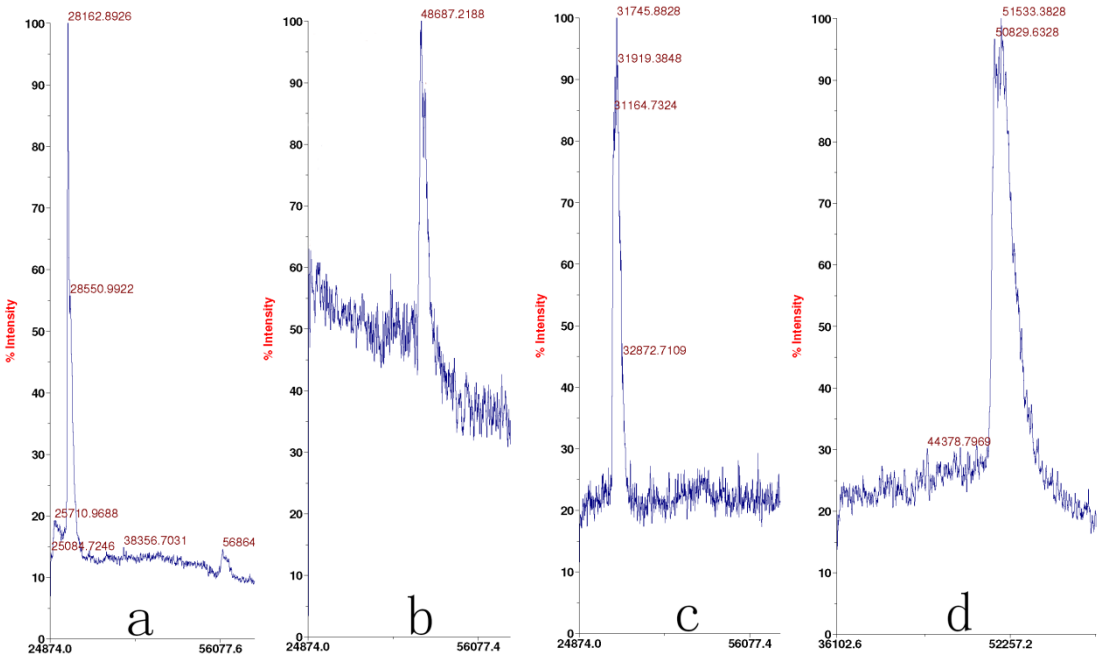

Figure S1. MALDI-TOF analyzed molecular weight of ELP[V_5-70](a), PEG-ELP[V_5-70] (b), ELP[VH_4-70](c) and PEG-ELP[VH_4-70] (d).

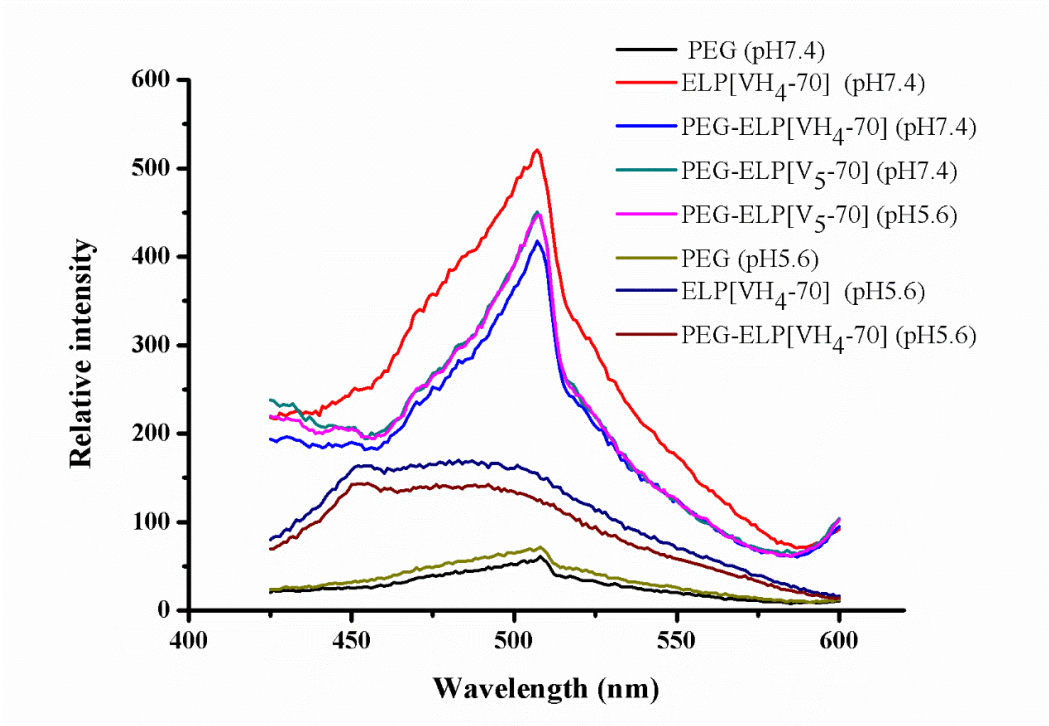

Figure S2. ANS analyzed hydrophobicity of PEG, ELP and PEG-ELP.

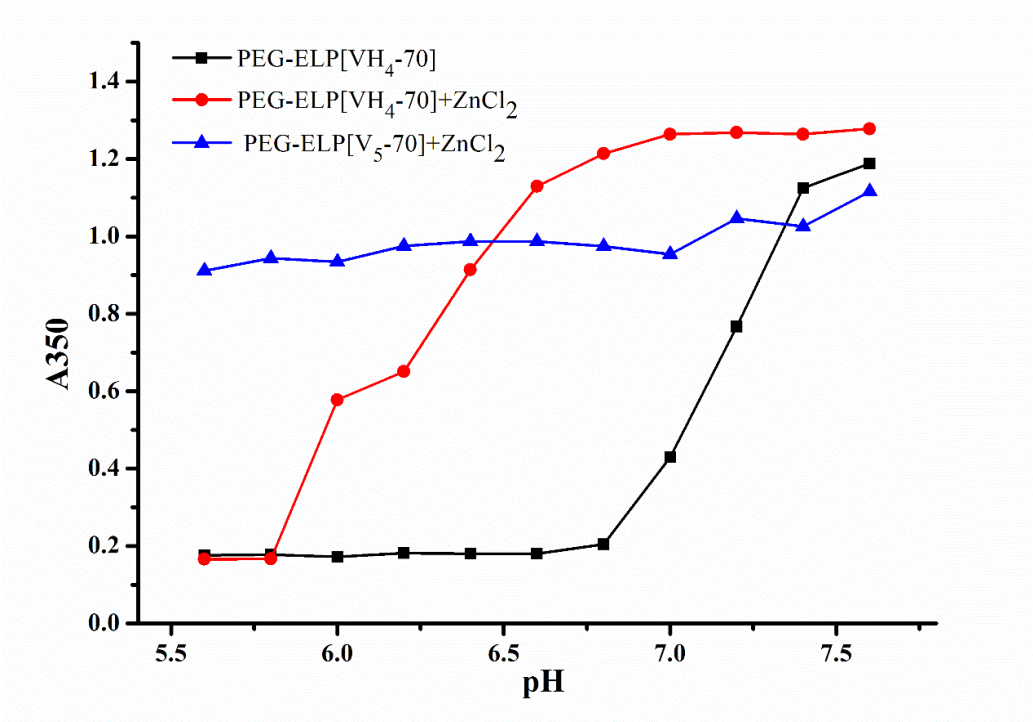

Figure S3. Material properties of histidine-rich ELPs and PEG-ELP. Turbidimetry (A350) was measured over a range of pH.

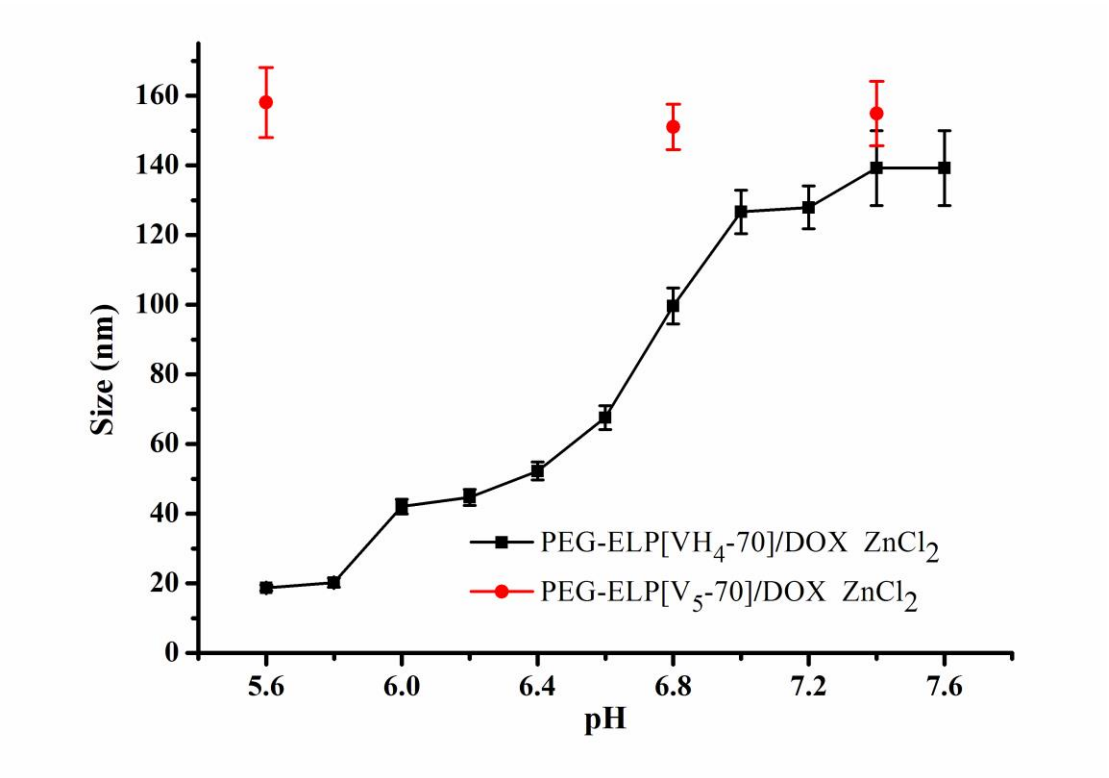

Figure S4. Hydraulic radius was measured with different pH, presenting 50μM $ZnCl_2$ (37 ^{o}C).

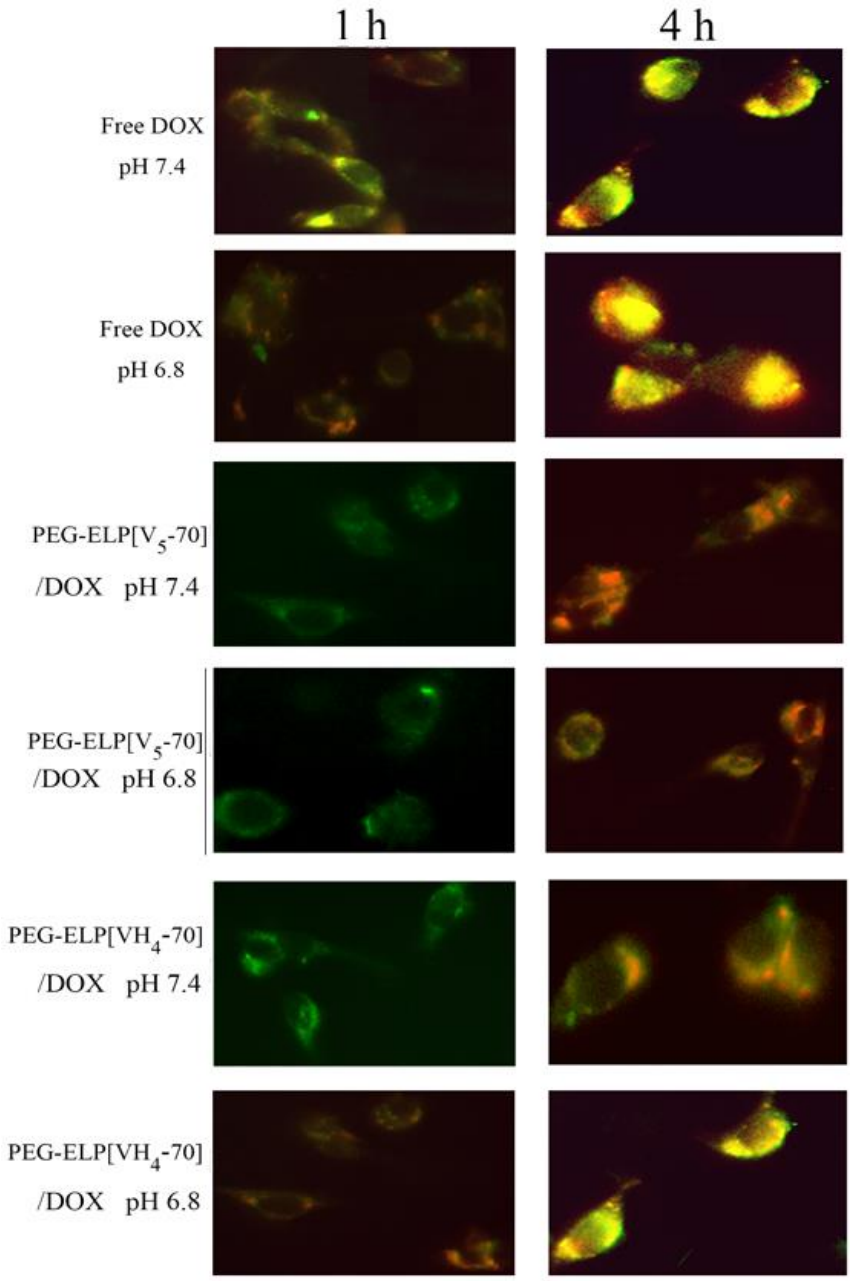

Figure S5. Intracellular release of DOX on CT-26 cells at different time (1, 4 h) observed by fluorescence microscopy. The lysosomes were stained by LysoTracker Green.

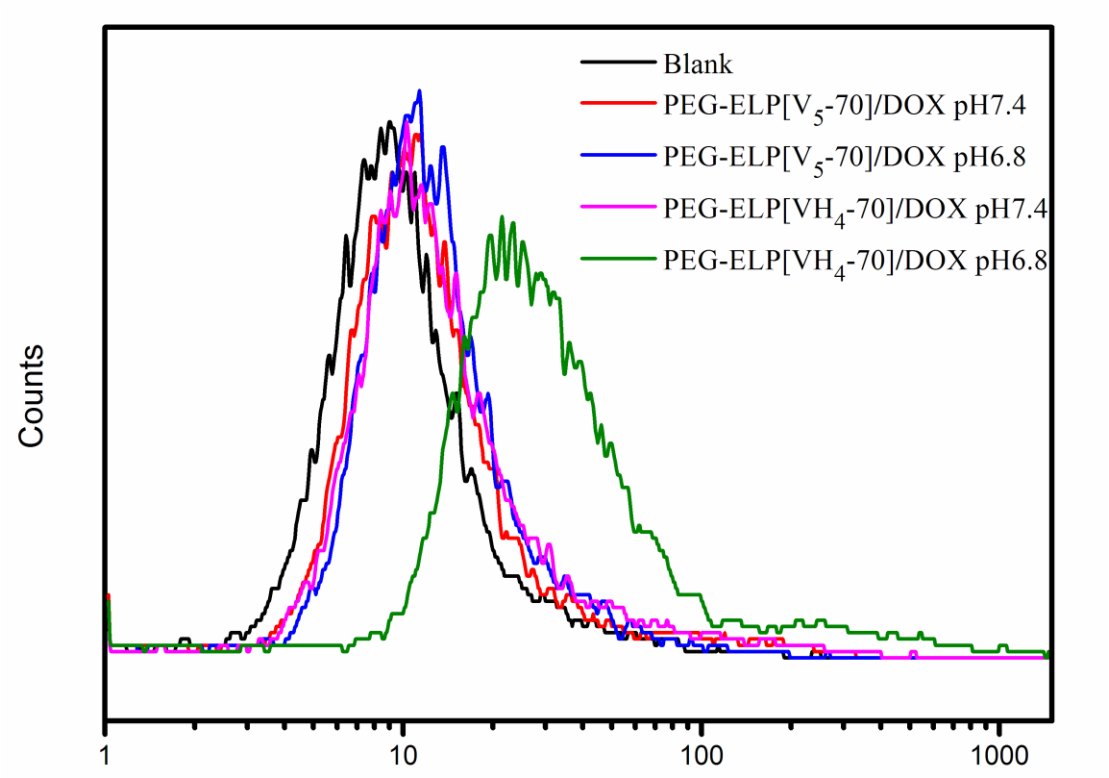

Figure S6. Cellular uptake of PEG-ELP/DOX on CT-26 cells.

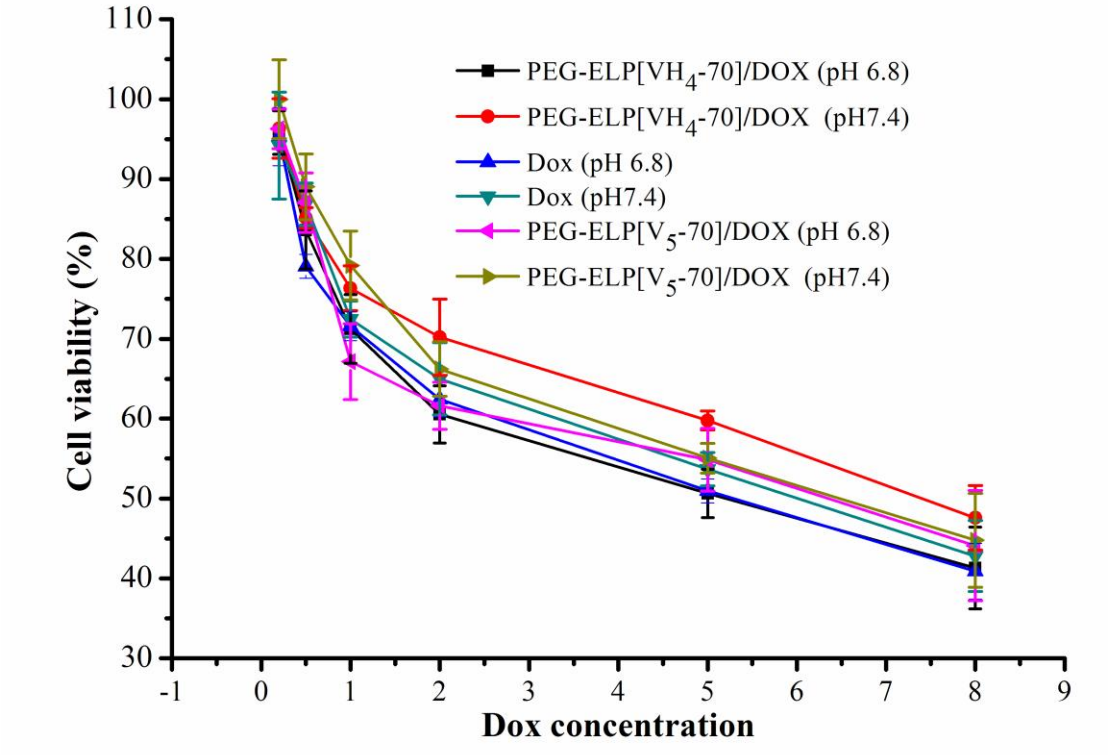

Figure S7. Effects of PEG-ELP/DOX and free DOX viability of CT-26. Cells were incubated with increasing concentrations of DOX in culture medium for 24 h. The proliferative response was then assessed by MTT.

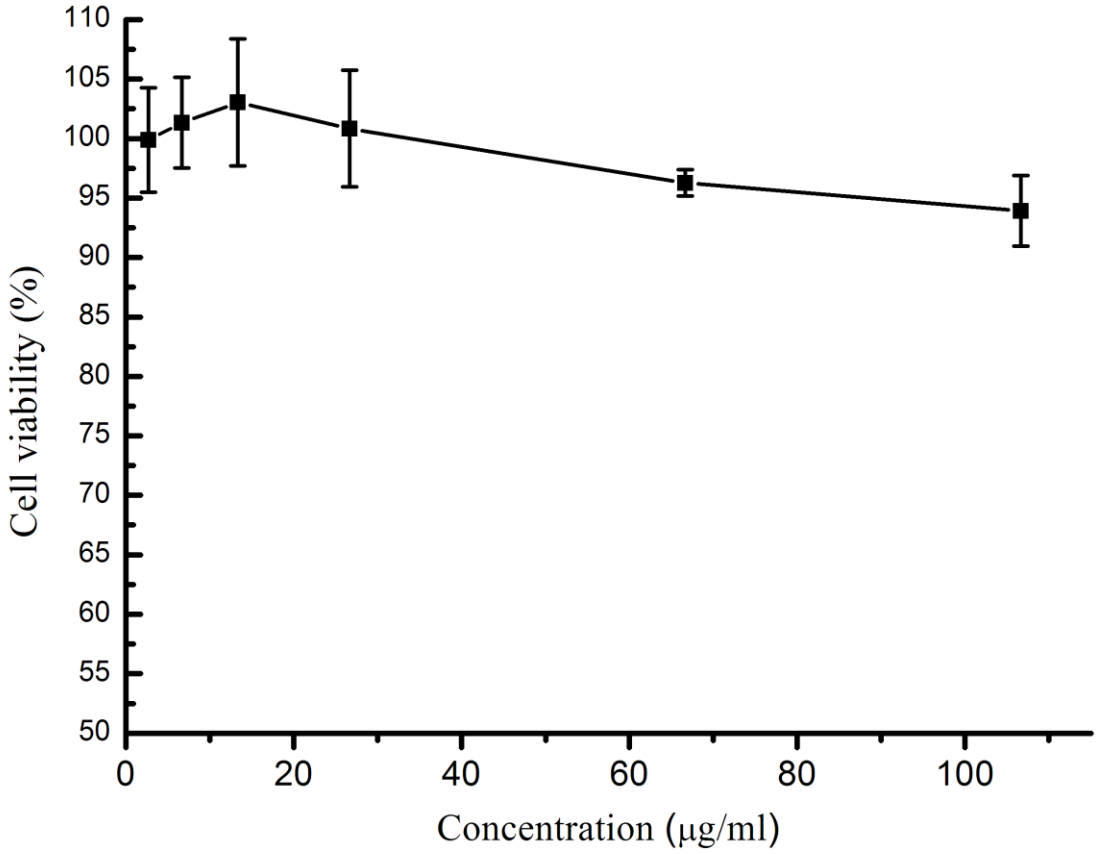

Figure S8. Effects of PEG-ELP viability of CT-26. Cells were incubated with increasing concentrations of PEG-ELP in culture medium for 24 h. The proliferative response was then assessed by MTT.

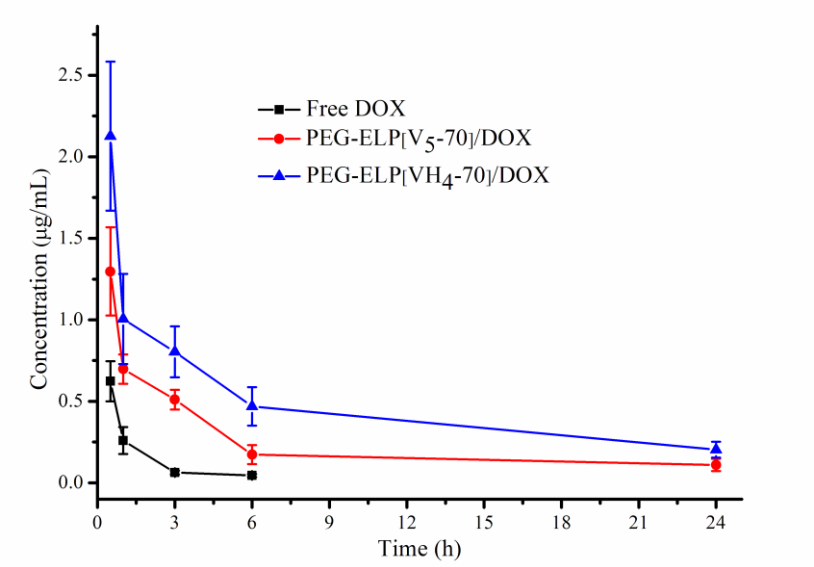

Figure S9. Plasma concentration-time profiles of DOX following i.v administration of Free DOX, PEG-ELP[V_5-70]/DOX and PEG-ELP[VH_4-70]/DOX (5mg/kg).

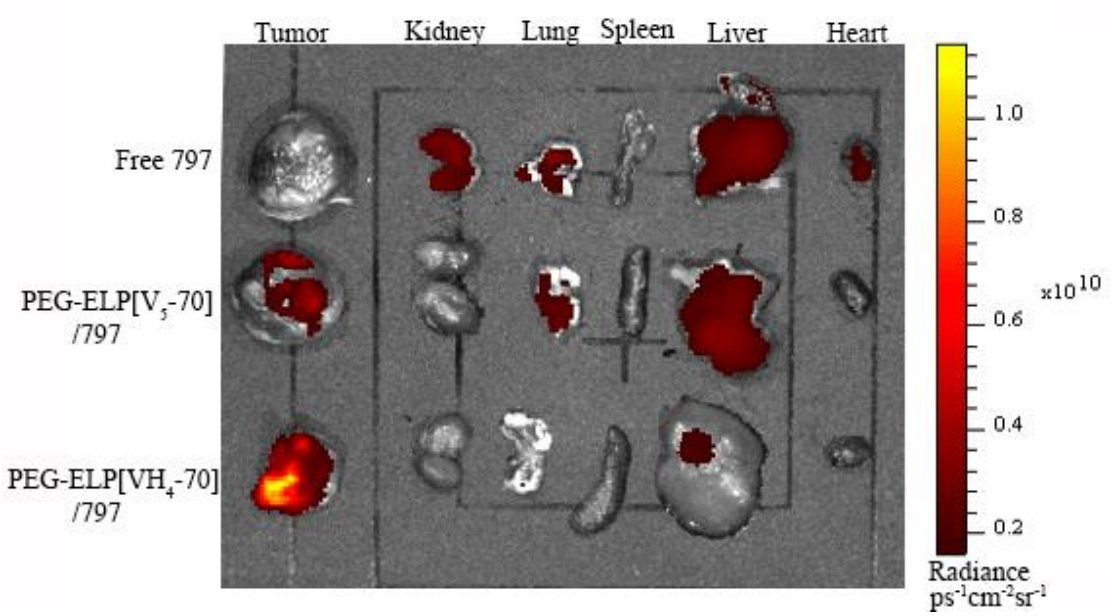

Figure S10. *Ex vivo* fluorescence imaging of the tumor and normal tissues harvested from the euthanized tumor-bearing BALB/c mice injection with different 797 fluorescent agent formulations.

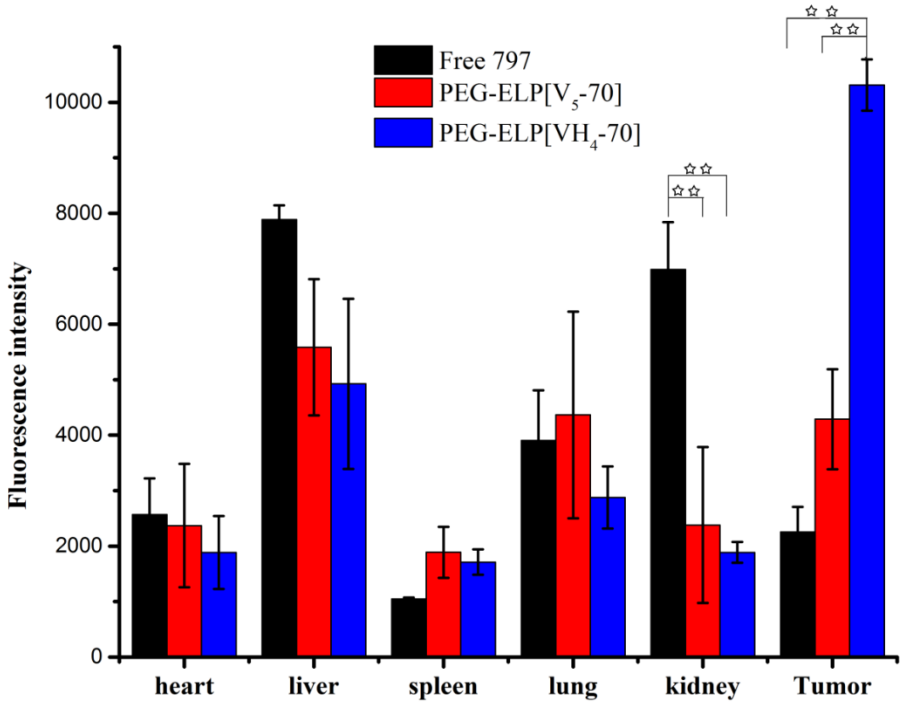

Figure S11. Quantification of fluorescent signal intensities of excised organs from mice at 24 h post injection. The data was recorded as total photons per centimeter squared per steradian (p/s/cm^2/sr).

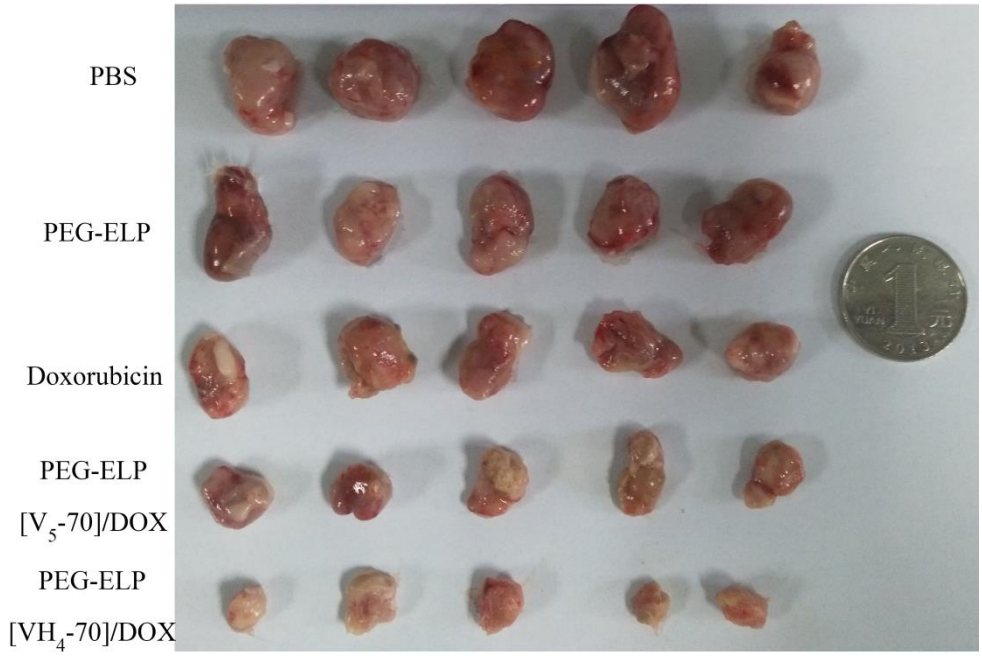

Figure S12. Animals were sacrificed 14 days after withdrawing administration and tumors were harvested and imaged.

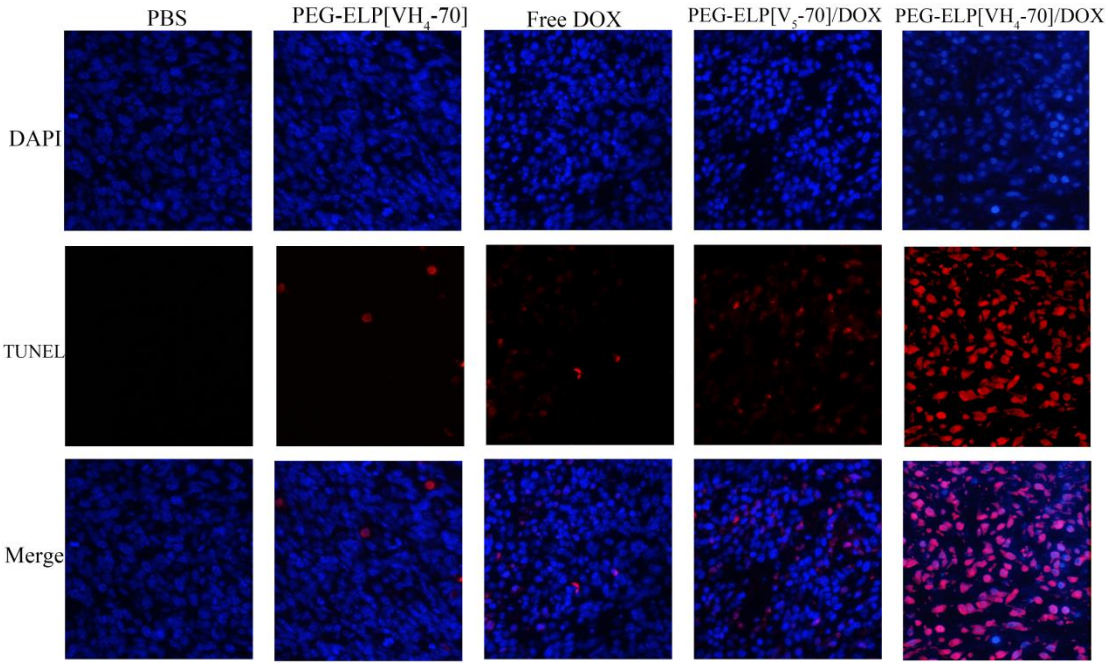

Figure S13. Tumor sections were immunostained with TUNEL staining for tumor cell apoptosis after treatment with different formulations.

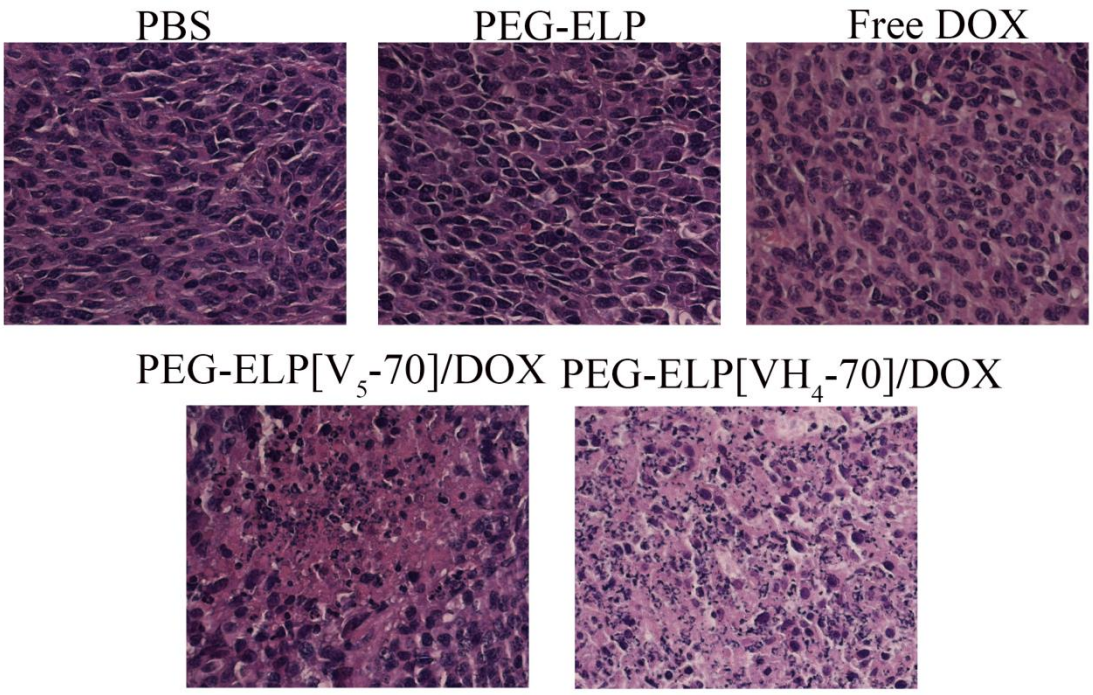

Figure S14. Hematoxylin-eosin (H&E) staining examination of tumor from the treated mice.

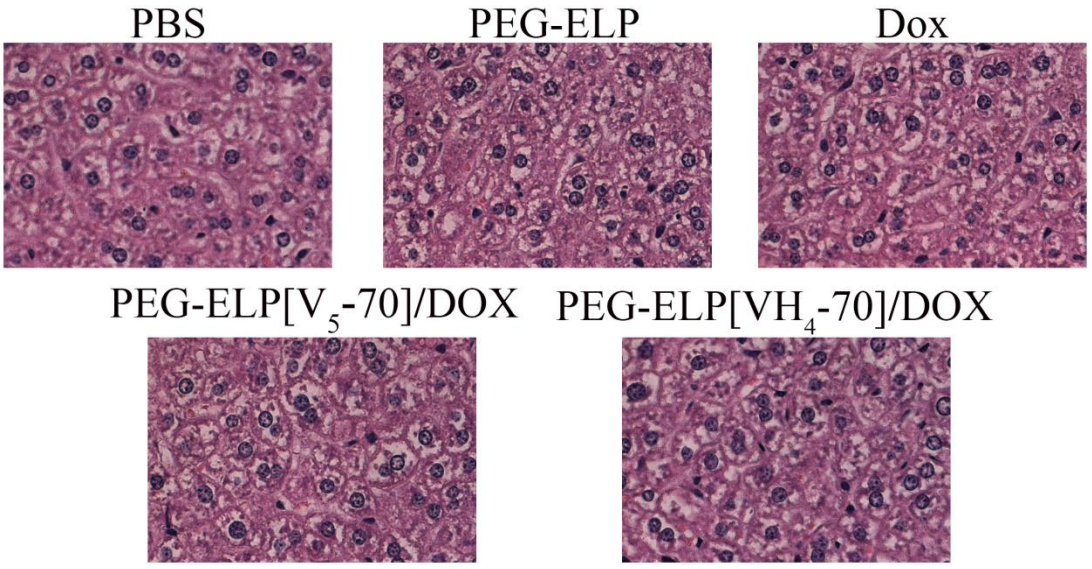

Figure S15. Hematoxylin-eosin (H&E) staining examination of liver from the treated mice.

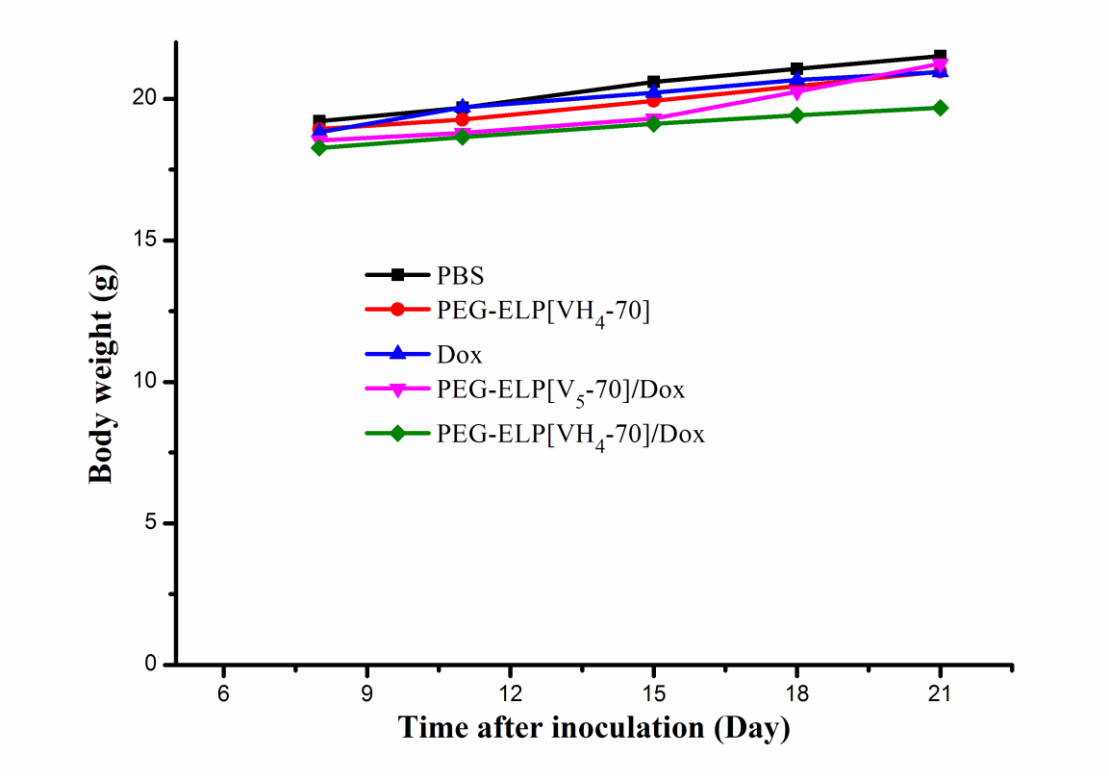

Figure S16. Body weight of each mouse in five groups was measured every three day. Results are expressed as mean ± S.D.

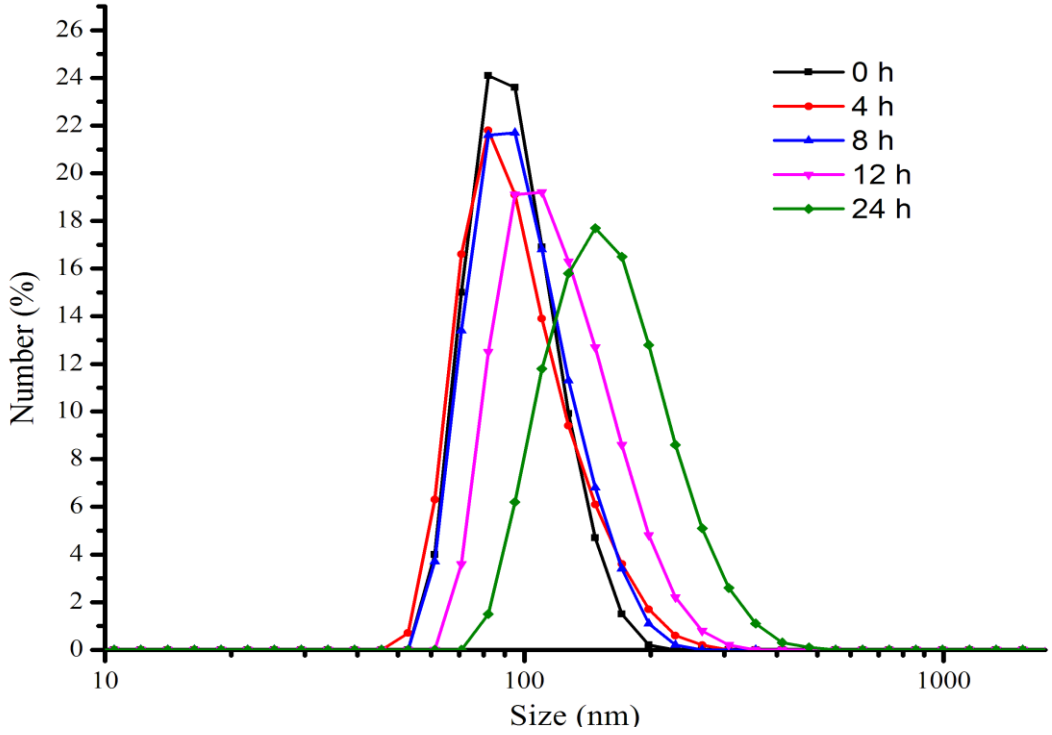

Figure S17. *In vitro* average diameter distribution of PEG-ELP[VH_4-70]/DOX over time.

Table S1: The pharmacokinetic analysis for PEG-ELP/DOX.

Pharmacokinetic parameter	Free DOX	PEG-ELP[V_5-70]/DOX	PEG-ELP[VH_4-70]/DOX
ACU_{inf}[a] (mg/L*h)	0.87±0.19	6.47±0.3*	13.64±2.58**
$T_{1/2}$[b](h)	1.56±0.14	7.03±0.93*	10.65±3.42*
CL[c](mL/h)	114.37±25.01	15.46±3.42*	7.32±0.76*

Values are means±s.d. [a]ACU_{inf}:(Area under the curve from zero to infinity) ; [b] $T_{1/2}$: Half-life; [c]CL: Clearance. *****P<0.05, ******P<0.01 *vs* Free DOX